Proceedings of the 2nd International Conference on Modern Medicine and Global Health
DOI: 10.54254/2753-8818/35/20240933

Bioinformatics-based analysis of the prognostic value of CAF-related genes in lung squamous cell carcinoma

He Siming[1], Gao Yizhou[1], Wu Zhihong[1,2]

[1]Department of Biological and Chemical Engineering, Zhejiang University of Science and Technology, Hangzhou, 310023, China

[2]wulab_zust@163.com

Abstract. The survival rate for lung squamous cell carcinoma (LUSC) is significantly lower compared to other types of tumors, although some effective immunotherapies have been applied in the clinic. The prognosis of LUSC is largely dependent on the individual patient's cancer assessment. Current clinical assessments based on clinical indicators and staging systems have limitations in accuracy. Therefore, prognostic prediction and assessment require precise and individualized assessment using genetic tools. Cancer-associated fibroblasts (CAFs) in the tumor microenvironment have been reported to impact the survival of LUSC by expressing specific proteins regulated by CAF-related genes (CAFRGs). Building upon this, the study aimed to identify CAFRGs in the gene expression data of LUSC using weighted gene co-expression network analysis (WGCNA), and one-way Cox and lasso regression screened for prognostically relevant CAFRGs in LUSC, incorporating six independent CAFRGs related to prognosis, to establish a risk score model for LUSC patients, and to further investigate potential CAF biomarkers related to LUSC prognosis. The TCGA database served as the training set, while the external dataset GSE30219 from the GEO database was employed for validating the accuracy and reliability of the model. Univariate Cox and multivariate Cox regression analyses demonstrated the significance of this risk score as a crucial independent prognostic factor for LUSC. According to immune infiltration and differences in immunotherapy response, personalized treatment strategies suitable for people with different risk scores were derived. We posit that the findings from this study offer robust evidence regarding the association between CAFRGs and LUSC prognosis. This can aid in establishing a dependable prognostic risk model, facilitating more precise prognostic predictions to guide personalized treatment decisions.

Keywords: Squamous cell carcinoma of lung, CAF, Prognosis, Model of risk

1. Introduction

Despite notable advancements in the treatment and management of lung cancer through contemporary medical interventions, lung cancer continues to be the predominant cause of cancer-related fatalities globally [1,2]. LUSC represents the second-largest subtype of lung cancer, as a subset of non-small cell lung cancer (NSCLC), it comprises around 30% of all lung cancer cases. [3]. LUSC often eludes early detection and is typically identified in intermediate to advanced stages, resulting in diminished 5-year survival rates [4] and consistently unfavorable prognostic outcomes. This is exacerbated by the absence of discernible driver mutations and a limited response to targeted therapy. Therefore, the exploration of prognostic markers for LUSC holds the potential to unveil more efficacious therapeutic strategies by

DOI: 10.54254/2753-8818/35/20240933

comprehending the prognostic risk and progression of LUSC patients. Presently, the prognostic risk for LUSC patients primarily relies on clinical assessments encompassing clinical indicators and staging systems. Nevertheless, this conventional staging approach exhibits constraints in predicting the survival and recurrence risks for individual LUSC patients [5,6]. It fails to facilitate precise, personalized assessments.

The treatment and prognosis of LUSC are intricately linked to the tumor microenvironment (TME), a decisive factor in cancer development and progression. The TME plays a pivotal role in influencing both tumor immunity and chemoresistance [7]. CAFs, a major component of the TME, exert influence over tumor cell growth, invasion, metastasis, angiogenesis, and chemoresistance through the secretion of various cytokines and matrix remodeling proteins [8-10]. Many studies have focused on CAFs, proposing a novel cancer treatment paradigm [11-13].

Recent studies have underscored the critical role of CAFs in the TME of LUSC in cancer development, progression, and prognosis. Multiple CAFRGs have been identified to correlate with LUSC survival. Notably, the consistent correlation of PDPN and α-SMA expression in CAFs of LUSC patients with low survival rates has been observed [14]. Moreover, fibroblast growth factor FGFR1 amplification has been identified as an early driving oncogenic event in LUSC [15]. FAP-α expression in CAFs is associated with microvessel and lymphatic vessel density in LUSC, suggesting its potential as a new prognostic biomarker [16]. Despite this, the therapeutic and prognostic value of characterizing CAFRGs for LUSC has been relatively understudied. Investigating the crosstalk between CAFRGs and the TME and establishing a more accurate prognostic model are crucial steps to unveil key pathways in the development and progression of LUSC. This approach can aid in providing individualized therapeutic strategies and prognostic assessments for patients.

In this study, we quantified CAFs and stromal cells in LUSC and assessed their prognostic effects using the "MCPcounter" and "Estimate" algorithms. Subsequently, CAFRGs were identified through WGCNA to explore their prognostic role in LUSC. Based on the identified prognostically relevant CAFRGs, a risk score model was developed for the prognostic prediction of LUSC patients. To ensure the model's predictive potential, TCGA data served as the training set, and LUSC data from GSE30219 in the external dataset GEO were used for validation. The prognostic significance of the CAFRGs risk scoring model in LUSC was further evaluated by establishing high and low-risk scoring groups, and individualized treatment protocols for different risk groups were derived by exploring associations and differences in various aspects of TME immune infiltration characteristics, immune checkpoints, and treatment responses.

2. Materials and methods

2.1. Data collection

RNA-Seq data and clinical information for LUSC patients were acquired from the TCGA database (https://portal.gdc.cancer.gov/), comprising 51 normal samples and 502 cancer samples. Clinical data encompassed details such as age, gender, survival status, survival time, and stage. The GSE30219 dataset, containing data from 61 LUSC patients along with clinical information, was retrieved from the GEO database (https://www.ncbi.nlm.nih.gov/geo/). Duplicate samples and those with missing follow-up information were excluded from the study. Quantitative scores for fibroblasts and stromal cells in the tumor of each sample were computed using the "MCPcounter" and "Estimate" algorithms.

2.2. Access to CAFRGs

WGCNA analysis [17] was employed to identify CAFRGs in LUSC. We constructed a weighted co-expression network based on the LUSC gene expression matrix using the R package "WGCNA". Subsequently, a soft threshold (β) was defined and utilized to establish a weighted adjacency matrix, reflecting the distribution of connected genes. The dynamic clipping algorithm was applied to the clustering tree, segmenting it based on gene relevance into distinct gene modules. Correlation analysis between the genes within each module and the fractions of mesenchymal fibroblasts and stromal cells

DOI: 10.54254/2753-8818/35/20240933

was computed using the Pearson test. Using this method, Pinpointed gene modules most relevant to fibroblasts and stromal cells. The Wilcoxon rank-sum test was then applied to identify differentially expressed genes associated with CAFs in both cancerous and adjacent tissues.

2.3. CAFRGs feature selection and prognostic risk model construction and validation

Prognostic features were developed using the TCGA training set, and their predictive performance was subsequently validated in the GEO validation set. To identify genes with prognostic significance, one-way Cox regression analysis was conducted on differentially expressed CAFRGs with a significance level of $P<0.05$. In order to mitigate overfitting, LASSO logistic regression analysis with ten-fold cross-validation was employed to further refine the selection of prognostic genes, particularly focusing on key CAFRGs. This process led to the development of a risk score model designed for predicting the prognosis of LUSC patients. The risk score, representing the expression level for each sample, was calculated based on the identified prognostic genes.

$$y_{risk\ score} = \sum_{i=1}^{n} (x_i \times z_i) \quad (1)$$

The expression n represents the count of CAFRGs.; $x_i$represents the expression corresponding to prognostic CAFRGs; and z_i is the corresponding coefficient determined by regression analysis. LUSC patients were stratified into low-risk and high-risk groups based on the median risk score. Survival disparities between these groups were assessed using Kaplan-Meier curves. The predictive performance of the prognostic model for clinical outcomes in LUSC patients was assessed by calculating the AUC of the ROC curve, considering sensitivity and specificity. Additionally, the external dataset GSE30219 was utilized to validate the robustness and precision of the developed model.

2.4. Independent Clinical Characterization of Risk Models Based on CAFRGs

Using risk scores and various clinical data, by conducting univariate Cox regression analysis and multivariate Cox regression analysis to investigate whether the risk score can serve as an independent indicator for Overall Survival (OS) in LUSC patients in the TCGA dataset.

2.5. Analysis of immune infiltration and immunotherapy

To assess the extent of infiltration for each immune cell type between the high and low-risk groups, an analysis was conducted using the CIBERSORT algorithm. Additionally, the levels of stroma and immune cell infiltration in the samples were analyzed utilizing the Estimate algorithm. Immunotherapy data specific to LUSC were obtained from the TIDE website (http://tide.dfci.harvard.edu). Population sensitivity to immunotherapy was further assessed between different risk groups using the "ggpubr" and "limma" R packages.

3. Results

3.1. WGCNA screening of CAF-related genes in squamous lung cancer

The "MCPcounter" and "Estimate" algorithms were utilized to compute quantitative scores for fibroblasts and stromal cells in each sample. Subsequently, survival differences between the low and high groups were analyzed using survival analysis. Optimal cutoffs for defining high and low groups were determined and are presented in Table 1. In TCGA, patients in the high CAFs group experienced a worse prognosis., with a significant difference noted ($P<0.05$), as illustrated in Figure 1A. Additionally, stromal cells, predominantly composed of fibroblasts and CAFs, were found to be a significant component of fibroblasts. Patients in the high stromal cell group also showed a poorer prognosis ($P<0.01$), as depicted in Figure 1B. These findings underscore the influential role of CAFs in impacting the prognosis of LUSC patients with statistically significant differences. Similar results were observed in the external validation set GSE30219, mirroring the TCGA findings. Patients in the high CAF and stromal cell groups exhibited a worse prognosis, with both demonstrating significant differences ($P<0.05$), as displayed in Figure 1C-D. The consistency between the results from the TCGA and the

DOI: 10.54254/2753-8818/35/20240933

external validation set reinforces the importance of investigating the prognostic role of CAFRGs in LUSC.

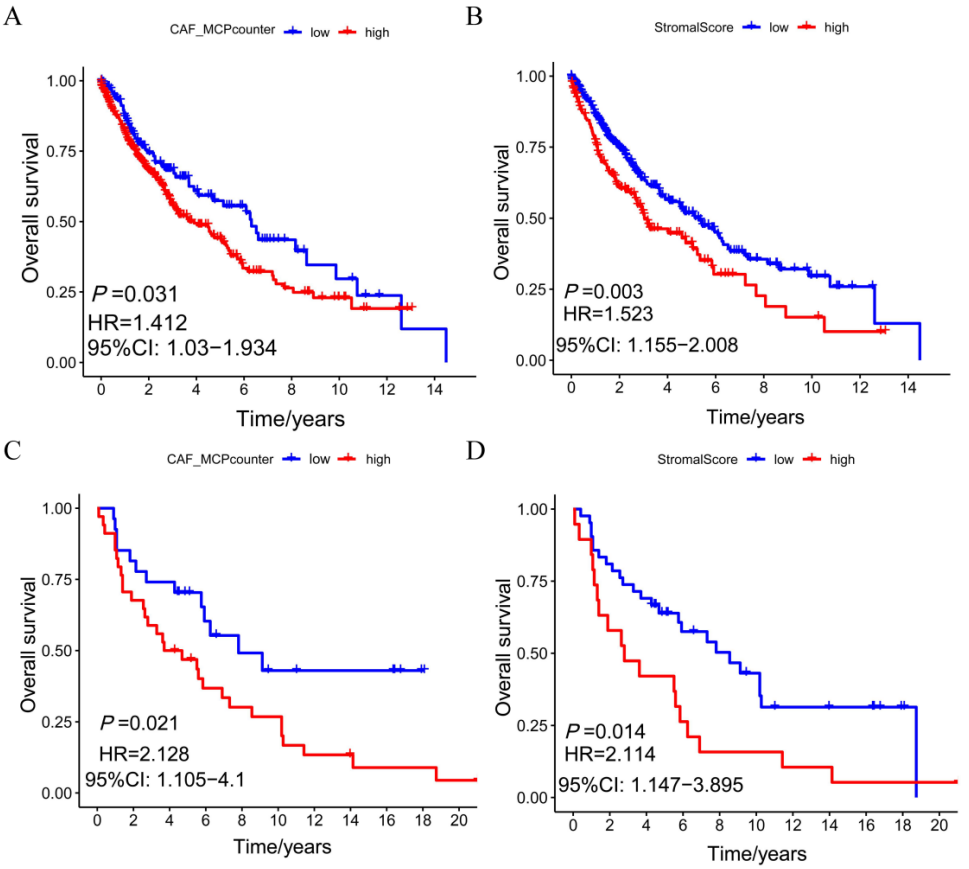

Figure 1. Survival analysis of CAF and stromal cell scores. Survival analysis of CAF score in TCGA; (B) Survival analysis of stromal cell score in TCGA; (C) Survival analysis based on CAF score in GEO; (D) Survival analysis by scoring stromal cells in GEO.

Table 1. Cutoff takes the value.

	TCGA	GEO
CAF-cutpoint	5.917 537	8.346 170
stromal cells-cutpoint	330.697 982	807.338 489

Based on the absolute median difference of gene expression, the top 5000 genes with the largest fluctuations were selected for WGCNA analysis. First, the missing values were checked so that the gene expression of each sample was greater than zero. Sample hierarchical clustering analysis was performed, and the nine samples with abnormal outliers were deleted for further analysis. Co-expression analysis of the above candidate genes was performed with respect to the infiltration of CAF and stromal cells by using the Pearson correlation coefficient. Next, the optimal choice of soft threshold was determined. The scale-free topology model was determined by calculating the connection strength between genes, setting the power index powers in the range of 1 to 20, and using the correlation coefficient R^2 in the interval 0 to 1. The soft threshold was determined based on the correlation coefficient R^2= 0.9, and the value 3 was considered the optimal value for constructing a hierarchical clustering tree (Figure 2A), where the gene distribution conformed to the scale-free network and the average connectivity tended to be stable. Next, a soft threshold value β=3 was chosen to calculate the neighbor-joining matrix of gene expression data in TCGA, the neighbor-joining matrix was transformed into a topological matrix, and the topological overlap was used to calculate the dissimilarity between genes. Finally, cluster analysis

DOI: 10.54254/2753-8818/35/20240933

was performed based on the dissimilarity between genes, and a systematic clustering tree was obtained. The number of genes in the gene module was set to be at least 30, and the dynamic clipping algorithm was used to cut the clustering tree according to the gene correlation and divide it into different gene modules. The gene modules were subjected to hierarchical clustering analysis to merge similar modules, and each color would have a corresponding gene module and a total of 10 gene modules were obtained according to the module clustering height was set to 0.2 (Figure 2B-C). The scoring files of CAF and stromal cells merged in TCGA, using cor function, were subjected to correlation analysis, and the blue module containing 928 genes was selected for subsequent predictive model construction, as it had the highest correlation coefficient with CAF (R=0.91, P<0.001) and stromal cells (R=0.73, P<0.001) (Figure 2D). By calculating GS and MM values and outputting scatter plots of modules related to and most importantly for CAF, 436 CAF-associated core genes were obtained based on the filtering conditions of MM=0.5 and GS=0.4 (Figure 2E). Finally, the analysis of variance was performed with the filter conditions set to P<0.05, |logFC|>1, and FDR<0.05. The results of the analysis of variance were obtained by Wilson's rank-sum test, and the analysis yielded a total of 231 CAF-associated variant genes (Figure 2F).

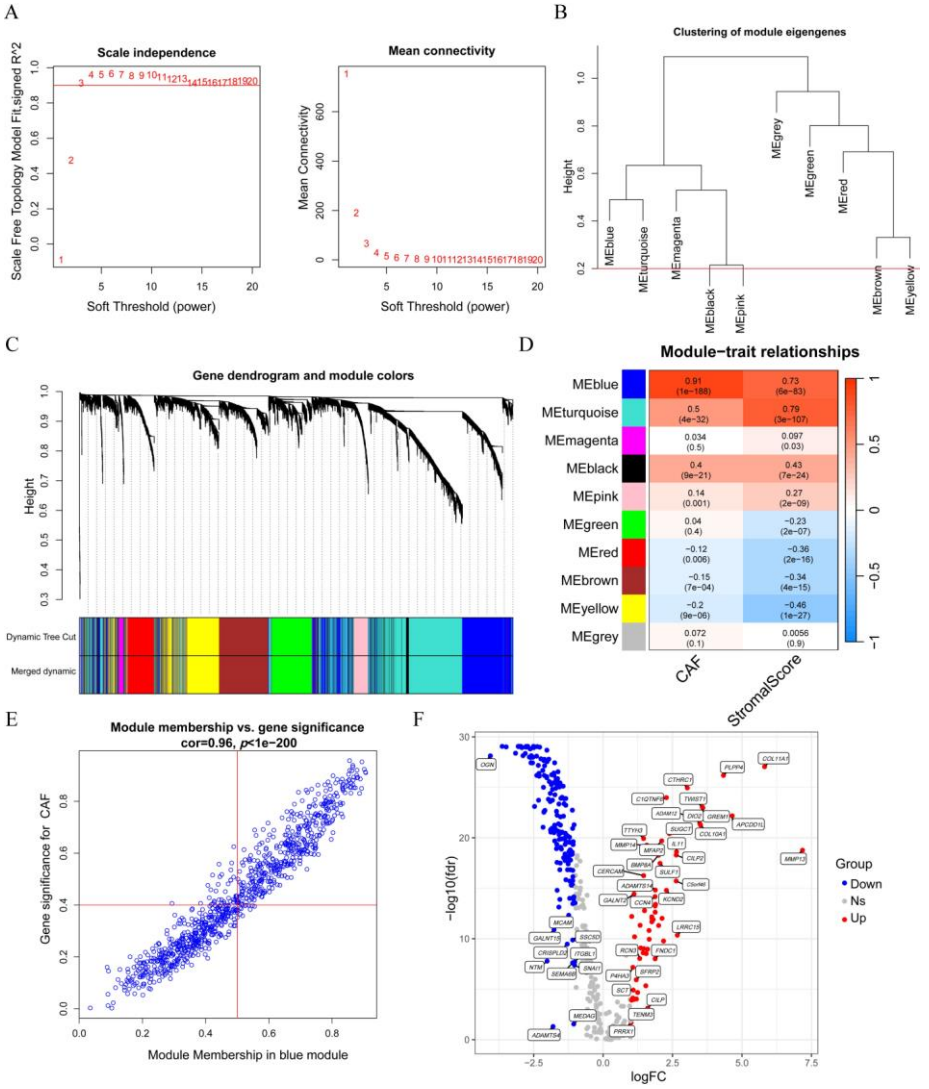

Figure 2. Screening of CAF associated genes. (A) soft threshold changes and mean connectivity; (B) Module cluster diagram; (C) dynamic splicing clustering tree; (D) Correlation heatmap of gene modules with CAF and stromal cells; (E) Scatter plot of correlation between blue module genes and CAF; (F) volcano map of differentially expressed genes.

DOI: 10.54254/2753-8818/35/20240933

3.2. Constructing a Risk Scoring Model Based on CAFRGs

From the 231 differentially expressed CAFRGs obtained by one-way Cox regression analysis using the Coxph function, 36 genes associated with OS were obtained from the initial screening by using the Coxph function to perform one-way Cox analysis and retaining significant gene variables (Figure 3A). Then, in order to avoid multicollinearity and overfitting of the 36 prognostically relevant CAF-characterized genes obtained by univariate Cox analysis, LASSO regression 10-fold cross-validation was used to further screen the prognostically relevant CAFRGs and develop the prognostic risk scoring model, and six CAFRGs were finally identified and included in the risk scoring model as shown in Figure 3B-C. Their risk coefficients are shown in Table 2.

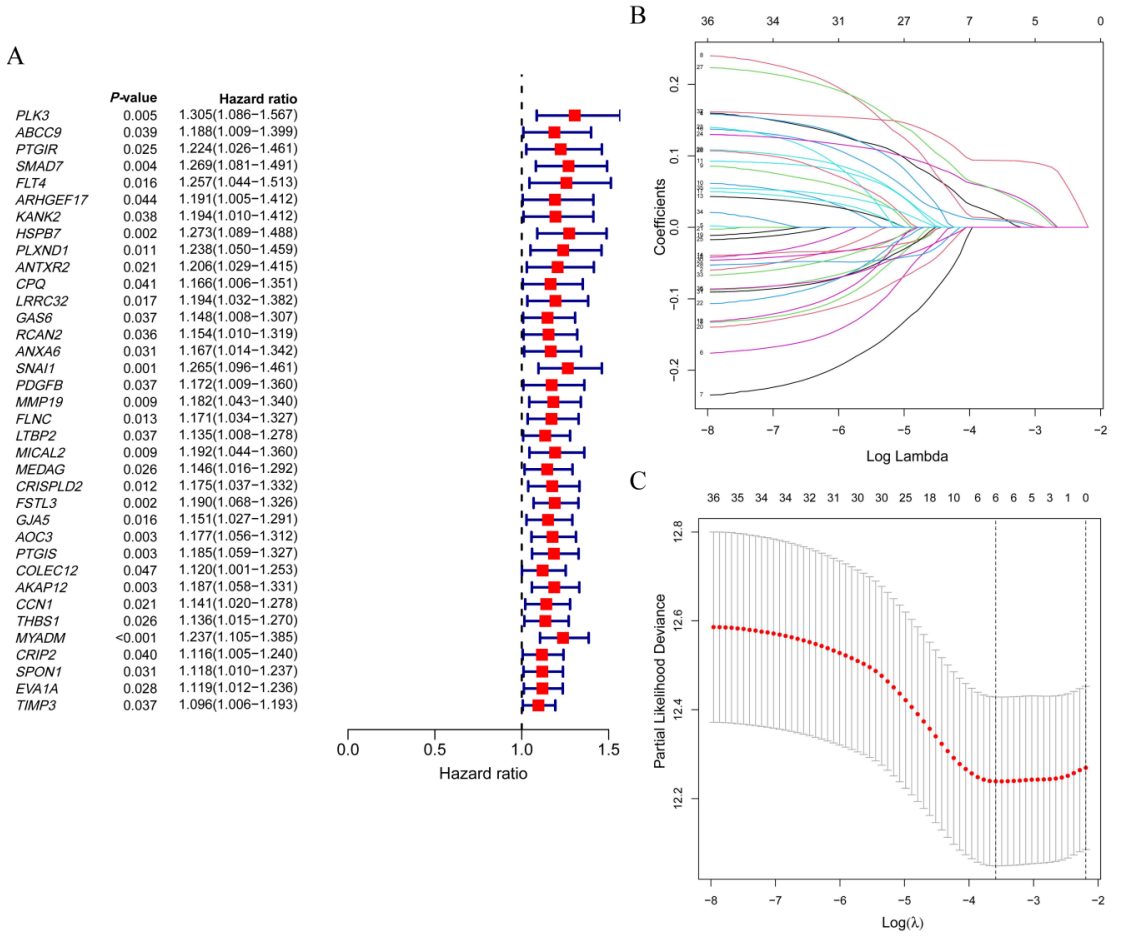

Figure 3. Six CAFRGs were selected for prognostic model construction. (A) univariate Cox analysis; (B) partial regression coefficient plot; (C) partial likelihood deviation plot.

Table 2. Coefficient of risk.

Gene	Coef
PLK3	0.017 030 650
HSPB7	0.011 989 487
SNAI1	0.009 710 459
FSTL3	0.052 542 346
PTGIS	0.051 581 356
MYADM	0.093 495 470

DOI: 10.54254/2753-8818/35/20240933

Using the risk score formula (1), the gene expression was multiplied by the risk factor to obtain the risk score. Patients were divided into high-risk (n=247) and low-risk (n=248) groups using the median risk score as the threshold. Kaplan-Meier survival curves were used to compare the survival differences between the high- and low-risk groups, and in TCGA, the high-risk group exhibited shorter OS compared to the low-risk group (P<0.001). (Figure 4A). The same results as in the training set were also observed in the GSE30219 validation set through the validation of GEO data, with poorer prognosis in the high-risk group (P<0.05) (Figure 4C). Thus, the accuracy and reliability of the constructed prognostic risk scoring model for CAF-related genes in lung squamous carcinoma were verified. The sensitivity and specificity of the prognostic model for predicting clinical outcomes in patients with squamous lung cancer were analyzed by calculating the AUC of the ROC curve. The AUC at 3, 4, and 5 years in the TCGA training set is shown in Figure 4B, and the AUCs at 3, 4, and 5 years in the GEO validation set are shown in Figure 4D; the AUC is the area under the curve of the ROC curve, and it takes the value of 0.1 and 1, and the bigger the better, and the better the predictive value if the AUC>0.6. The AUC ranges from 0.1 to 1 in the ROC curve. An AUC>0.6 suggests a good predictive value, indicating that the CAFRGs prognostic risk model has a strong ability to predict the prognosis of squamous carcinoma and can serve as a reliable prognostic indicator.

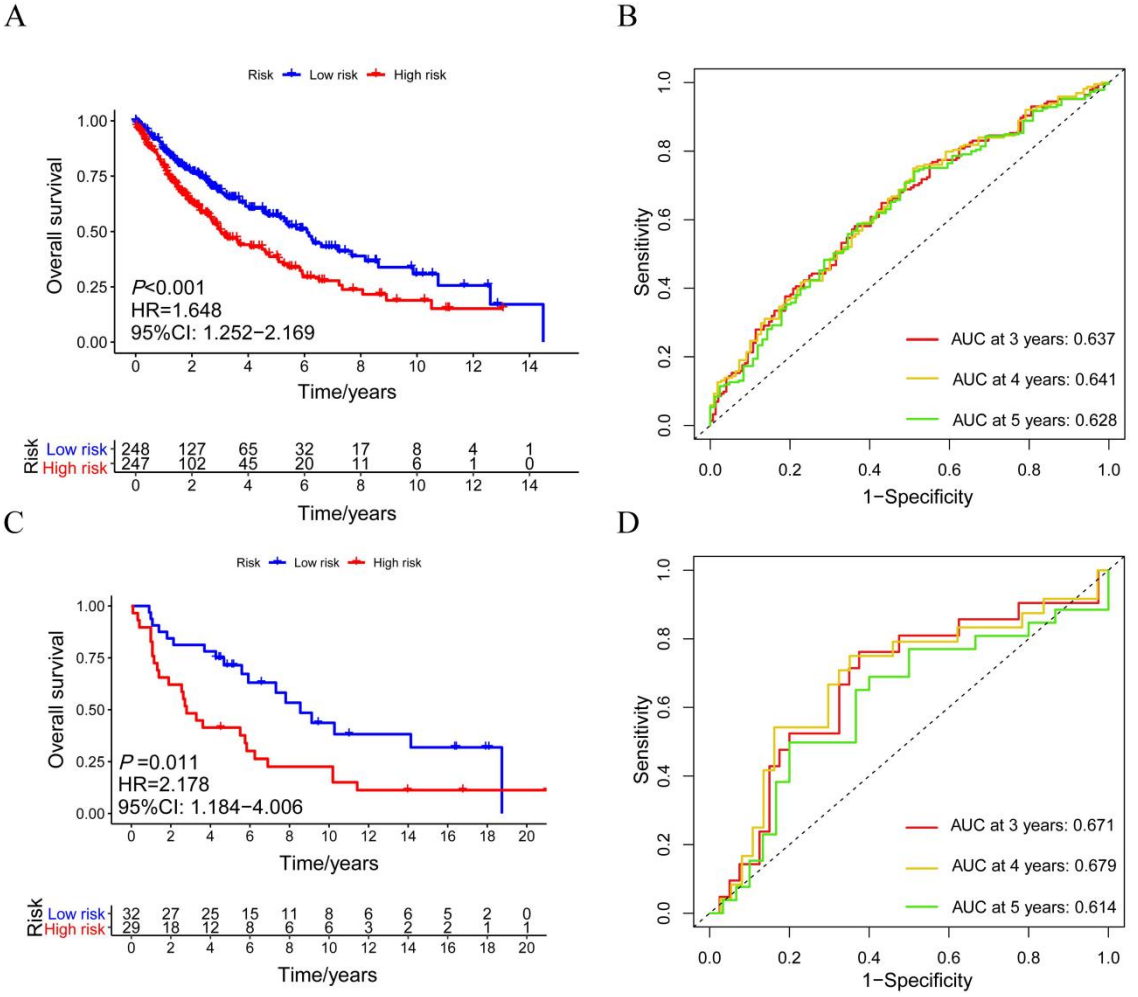

Figure 4. Evaluation of prognostic models. (A) survival analysis in TCGA training dataset; (B) ROC curves at 3, 4, and 5 years in TCGA; (C) survival analysis in GSE30219 validation set; (D) ROC curves of 3, 4 and 5 years in GSE30219 validation set.

DOI: 10.54254/2753-8818/35/20240933

3.3. Independent prognostic analysis of risk models based on CAFRGs

Univariate and multivariate Cox analyses incorporated factors such as age, gender, pathological stage, and risk score. The results indicated that the risk score (P<0.001) was a prognostic factor (Figure 5A), and the risk score (P<0.001) served as an independent predictor of prognosis (Figure 5B). Thus, the CAFRGs risk score can function as an independent prognostic factor for LUSC. Survival analysis was conducted on the six CAFRGs involved in constructing the prognostic risk score model. The findings demonstrated poorer prognosis in the high-expression group for all six CAFRGs, as depicted in Figure 5C, with statistically significant differences between the high and low expression groups. This suggests their potential as independent prognostic markers for LUSC.

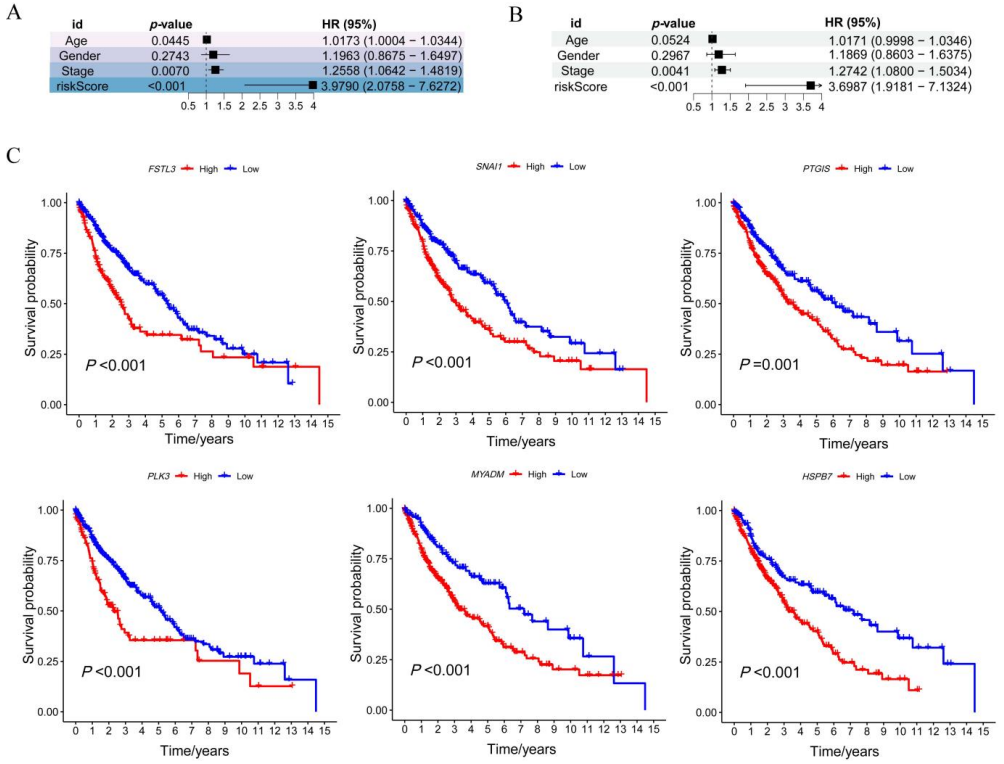

Figure 5. Independent prognostic assessment of prognostic models. (A) One-way Cox regression analysis of the prognostic risk model; (B) Multifactorial Cox regression analysis of the prognostic risk model; (C) Survival analysis of the 6 CAFRGs involved in the prognostic model construction.

3.4. Immune Infiltration Analysis and Immunotherapy Analysis Based on Risk Model Characteristics of CAFRGs

Due to the close association between CAF and the TME, immune analysis was conducted using the CIBERSORT algorithm to explore differences in TME immune infiltration characteristics between the two risk groups. As shown in Figure 6A, significant differences were observed in the infiltration scores of 9 out of 22 immune cells between different risk groups. Figure 6B revealed that 6 features of CAFRGs were associated with immune cell infiltration. Further investigation into the correlation between immune infiltration features and high/low-risk groups involved using the ESTIMATE algorithm to calculate sample immune scores, stromal scores, and overall ESTIMATE scores. The results, as presented in Figure 6C, demonstrated significantly higher stromal scores and immune cell levels in the high-risk groups. These findings suggest a close relationship between risk scores based on CAFRGs and the tumor immune microenvironment. Considering the clinical importance of immune checkpoint inhibitors, typical immune checkpoints, including PDCD1, CD274, CTLA4, POLE2, FEN1, MCM6, POLD3, MSH6, MSH2, FAP, TAGLN, and LOXL2, were further analyzed to correlate with risk scores (Figure 6D). The analysis revealed positive correlations of PDCD1, CTLA4, FAP, TAGLN, and LOXL2 with

DOI: 10.54254/2753-8818/35/20240933

risk scores, while POLE2, FEN1, MCM6, MSH6, and MSH2 exhibited negative correlations. Subsequently, The TIDE algorithm was employed to evaluate the potential therapeutic effectiveness of immunotherapy in both high- and low-risk patient groups. Higher TIDE predictive scores suggest a higher probability of immune evasion, suggesting a lower likelihood of benefiting from immunotherapy. Figure 6E illustrates that patients in the high-risk group exhibited higher TIDE scores compared to those in the low-risk group, implying that patients in the low-risk group may potentially derive greater benefits from immunotherapy. This information can guide physicians in making individualized therapy decisions.

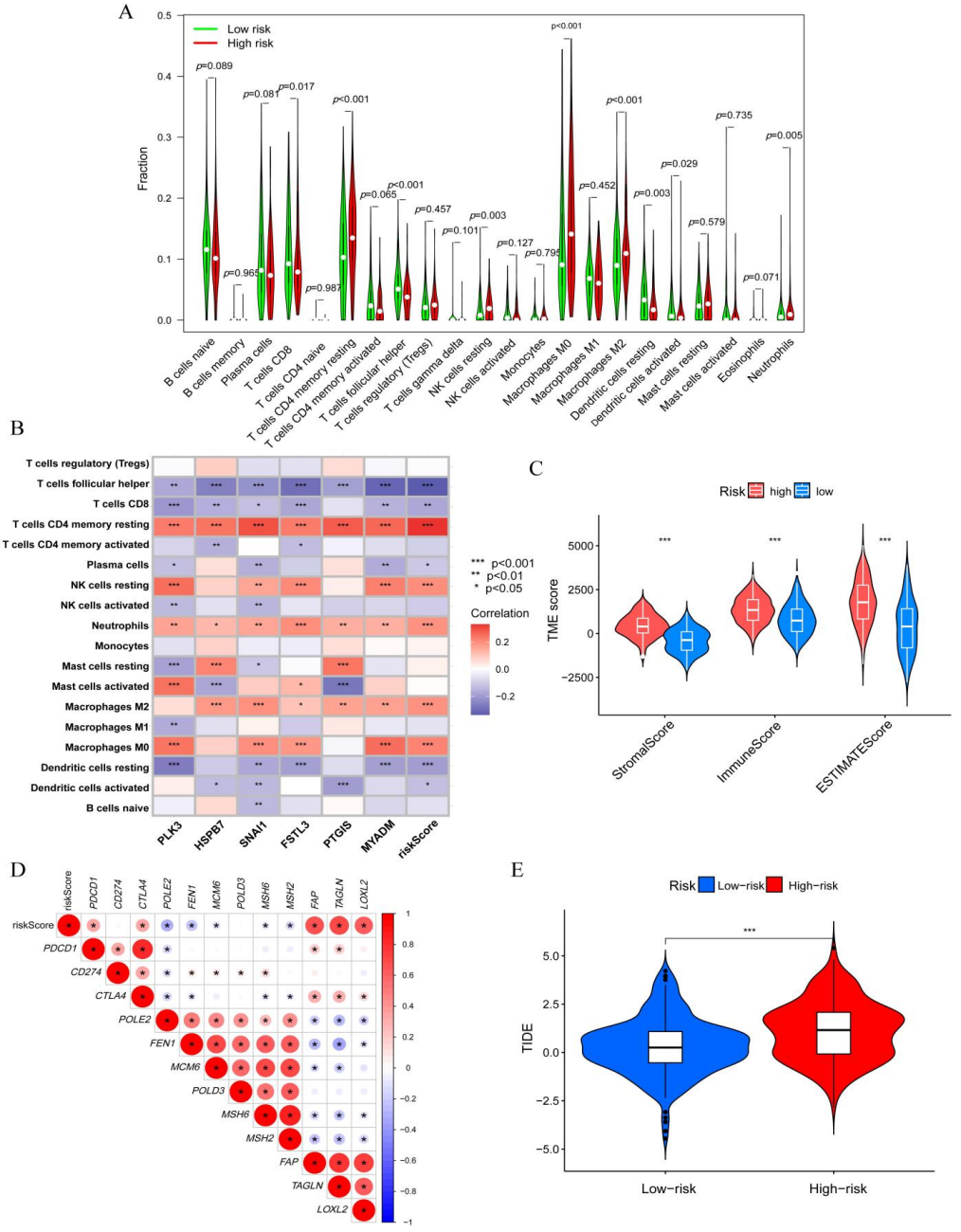

Figure 6. Correlation analysis between immune cells and characteristics of CAFRGs and immunotherapy analysis. denoted by *** (P<0.001), ** (P<0.01), and * (P<0.05). (A) assessment of immune cell infiltration in high and low-risk groups; (B) Correlation analysis between six CAFRGs and immune cells; (C) ESTIMATE was utilized to calculate the tumor microenvironment score; (D) immune checkpoint correlation analysis; (E) Immunotherapy analysis.

DOI: 10.54254/2753-8818/35/20240933

4. Discussion

CAF regulates cancer progression by modulating ECM and cancer cell adhesion. The TME is very complex in cancer patients. Previous research has primarily emphasized immune cells, yet the interaction between CAFs and other cells remains inadequately understood. CAF isolated from various tumors exhibit greater secretory capacity, propensity to proliferate, and metabolically active than normal fibroblasts [18]. CAF has been found in many cancers and plays a unique role therein, demonstrating its heterogeneity [19]. Targeting CAFRGs for LUSC analysis offers fresh insights into the prognosis and treatment of LUSC patients.

The study categorized LUSC patients into high and low score groups based on quantitative CAF and stromal cell scores. A significant difference in survival prognosis was observed between the high and low groups, with the high score group having a poorer prognosis. This underscores the importance of investigating CAFRGs in LUSC prognosis. Through WGCNA, genes highly correlated with CAF in LUSC were identified. Differential analysis and subsequent one-way Cox and lasso regression were employed to characterize CAFRGs associated with LUSC prognosis. The resulting prognostic risk score model, based on six screened CAFRGs, demonstrated longer OS in the low-risk group compared to the high-risk group, validated in an external GEO dataset. The risk score model emerged as an independent prognostic factor for LUSC, offering implications for prognostic and treatment decisions. The six CAFRGs (PLK3, HSPB7, SNAI1, FSTL3, PTGIS, and MYADM) implicated in the risk score model play roles in cancer progression. PLK3, a serine-threonine kinase, enhances oncogenicity in the mutant P53 pathway [20]. PLK3 exhibits a negative correlation with the TP53 mutation status in LUSC [21]. HSPB7, a potential tumor suppressor, inhibits LUAD cell proliferation, migration, and invasion [22,23]. its specific role in LUSC remains unclear. SNAI1, a zinc-finger transcription factor, is a driver of cancer progression and is correlated with increased tumor cell migration and lung cancer metastasis [24,25]. FSTL3 is identified as a novel oncogene in NSCLC, serving as a valuable therapeutic target [26]. PTGIS promotes LUSC proliferation, migration, and invasion, suggesting its potential as a therapeutic target and prognostic biomarker [27]. which was also demonstrated again in the present study. MYADM belongs to the MAL family of integral membrane proteins. Utilizing MAL-family proteins as cancer biomarkers can provide valuable prognostic and diagnostic insights for various human cancers [28]. Previous studies have indicated that MYADM serves as an independent prognostic factor in patients with NSCLC [29], which is also highlighted in the present study. The new prognostic biomarkers associated with CAF screened by the study can be used to find new therapies for LUSC patients.

The intricate interplay between various immune and stromal cells, leading to immunosuppressive interactions within the TME in LUSC, is closely associated with patient prognosis [30]. his study comprehensively analyzed immune cell infiltration in the TME, unveiling significant differences in stromal and immune scores between low-risk and high-risk groups. These differences were correlated with distinct prognoses. Patients in the high-risk group exhibited heightened infiltration of T-CD4 memory resting cells, NK resting cells, macrophage M0, macrophage M2, and neutrophils, indicating a potentially immunosuppressive TME. T-CD4 memory resting cells, known for their role in initiating anti-tumor immunity [31], were notably more prevalent in the high-risk group. Conversely, patients in the low-risk group showed increased presence of T-CD8 cells, helper follicular T cells, dendritic resting cells, and dendritic activated cells, suggesting a more favorable immune landscape. Previous studies have highlighted the impact of CAF-induced reactive oxygen species (ROS) on myeloid suppressor cells (MDSC) in LUSC, with potential implications for T-CD8 cell proliferation [32]. However, the connection between CAF and numerous other immune cells in LUSC is uncertain. Immunotherapeutic approaches in the clinic, primarily targeting current markers, have demonstrated limited efficacy in advanced LUSC patients [33]. Therefore, in this study, a notable difference was observed in the immunotherapy scores between patients in the high-risk group and those in the low-risk group. The high-risk group might be more prone to immune escape, while patients in the low-risk group could potentially exhibit a more favorable response to immunotherapy. The findings of the above study may help to personalize immunotherapy and improve treatment outcomes. This study may have several limitations. First, the study relied only on data from public sources, which may involve selection bias.

DOI: 10.54254/2753-8818/35/20240933

Second, future experimental studies should be conducted to confirm the detailed molecular processes by which CAFRGs crosstalk with CAF and other cells. Finally, further clinical studies should be conducted to validate the prognostic model relying on the six CAFRGs.

5. Conclusion

In conclusion, a prognostic risk model based on CAFRGs can serve as an independent prognostic factor for LUSC. six genes, PLK3, HSPB7, SNAI1, FSTL3, PTGIS, and MYADM, can be used as prognostic biomarkers for LUSC. These findings provide reliable evidence for the relationship between CAFRGs and LUSC prognosis, and offer the possibility of further development of individualized treatment for LUSC.

Acknowledgments

This study was co-sponsored by the National Natural Science Foundation of China (Grant no: 81972922).

References

[1] Sung H, Ferlay J, Siegel R L, Laversanne M, Soerjomataram I, Jemal A; Bray F, 2021, Global cancer statistics 2020: GLOBOCAN estimates of incidence and mortality worldwide for 36 cancers in 185 countries, Ca-a Cancer Journal for Clinicians, 71: 209-249.

[2] Siegel R L, Miller K D, Fuchs H E; Jemal A, 2022, Cancer statistics, 2022, Ca-a Cancer Journal for Clinicians, 72: 7-33.

[3] Xu F, Lin H, He P, He L, Chen J, Lin L; Chen Y, 2020, A TP53-associated gene signature for prediction of prognosis and therapeutic responses in lung squamous cell carcinoma, Oncoimmunology, 9(1): 1731943.

[4] Lai Y-H, Chen W-N, Hsu T-C, Lin C, Tsao Y; Wu S, 2020, Overall survival prediction of non-small cell lung cancer by integrating microarray and clinical data with deep learning, Scientific Reports, 10(1): 4679.

[5] Lian S, Liu Z, Zhou Y, Guo J, Gong K; Wang T, 2020, The differential expression patterns and co-expression networks of paralogs as an indicator of the TNM stages of lung adenocarcinoma and squamous cell carcinoma, Genomics, 112: 4115-4124.

[6] Zeng Z, Yang F, Wang Y, Zhao H, Wei F, Zhang P, Zhang X; Ren X, 2020, Significantly different immunoscores in lung adenocarcinoma and squamous cell carcinoma and a proposal for a new immune staging system, Oncoimmunology, 9(1):1828538

[7] Hanahan D; Weinberg R A, 2011, Hallmarks of cancer: the next generation, Cell, 144: 646-674.

[8] Mao X, Xu J, Wang W, Liang C, Hua J, Liu J, Zhang B, Meng Q, Yu X; Shi S, 2021, Crosstalk between cancer-associated fibroblasts and immune cells in the tumor microenvironment: new findings and future perspectives, Molecular Cancer, 20(1):131.

[9] Li Y, Chen Y, Miao L, Wang Y, Yu M, Yan X, Zhao Q, Cai H, Xiao Y; Huang G., 2021, Stress-induced upregulation of TNFSF4 in cancer-associated fibroblast facilitates chemoresistance of lung adenocarcinoma through inhibiting apoptosis of tumor cells, Cancer Letters, 497: 212-220.

[10] Wu X, Zhou Z, Xu S, Liao C, Chen X, Li B, Peng J, Li D; Yang L, 2020, Extracellular vesicle packaged LMP1-activated fibroblasts promote tumor progression via autophagy and stroma-tumor metabolism coupling, Cancer Letters, 478: 93-106.

[11] De P, Aske J; Dey N, 2021, Cancer-associated fibroblast functions as a road-block in cancer therapy, Cancers, 13(20): 5246.

[12] Slany A, Bileck A, Muqaku B; Gerner C, 2015, Targeting breast cancer-associated fibroblasts to improve anti-cancer therapy, Breast, 24: 532-538.

[13] Shintani Y, Kimura T, Funaki S, Ose N, Kanou T; Fukui E, 2023, Therapeutic targeting of cancer-associated fibroblasts in the non-small cell lung cancer tumor microenvironment, Cancers, 15(2): 335.

DOI: 10.54254/2753-8818/35/20240933

[14] Irvine A F, Waise S, Green E W, Stuart B; Thomas G J, 2021, Characterising cancer-associated fibroblast heterogeneity in non-small cell lung cancer: a systematic review and meta-analysis, Scientific Reports, 11(1): 3727.
[15] Craddock K J, Ludkovski O, Sykes J, Shepherd F A; Tsao M-S, 2013, Prognostic value of fibroblast growth factor receptor 1 gene locus amplification in resected lung squamous cell carcinoma, Journal of Thoracic Oncology, 8: 1371-1377.
[16] Chen L, Chen M, Han Z, Jiang F, Xu C, Qin Y, Ding N, Liu Y, Zhang T, An Z; Guo C, 2018, Clinical significance of FAP-α on microvessel and lymphatic vessel density in lung squamous cell carcinoma, Journal of Clinical Pathology, 71: 721-728.
[17] Zhang B, Horvath S, 2005, A general framework for weighted gene co-expression network analysis, Stat Appl Genet Mol Biol, 4: Article17.
[18] Kalluri R, 2016, The biology and function of fibroblasts in cancer, Nature Reviews Cancer, 16: 582-598.
[19] Ishii G, Ochiai A; Neri S, 2016, Phenotypic and functional heterogeneity of cancer-associated fibroblast within the tumor microenvironment, Advanced Drug Delivery Reviews, 99: 186-196.
[20] Vaughan C A, Singh S, Subler M A, Windle J J, Inoue K, Fry E A, Pillappa R, Grossman S R, Windle B, Yeudall W A, Deb S P; Deb S, 2021, The oncogenicity of tumor-derived mutant p53 is enhanced by the recruitment of PLK3, Nature Communications, 12(1):704.
[21] Deng S, Lu X, Zhang Z, Meng R, Li M; Xia S, 2021, Identification and assessment of PLK1/2/3/4 in lung adenocarcinoma and lung squamous cell carcinoma: Evidence from methylation profile, Journal of Cellular and Molecular Medicine, 25: 6652-6663.
[22] Naderi A, 2018, SRARP and HSPB7 are epigenetically regulated gene pairs that function as tumor suppressors and predict clinical outcome in malignancies, Molecular Oncology, 12: 724-755.
[23] Chen Z, Li P, Shen L; Jiang X, 2023, Heat shock protein B7 (HSPB7) inhibits lung adenocarcinoma progression by inhibiting glycolysis, Oncology Reports, 50(5): 196.
[24] Dong B; Wu Y, 2021, Epigenetic regulation and post-translational modifications of SNAI1 in cancer metastasis, International Journal of Molecular Sciences, 22(20): 11062.
[25] Wang X, Liu R, Zhu W, Chu H, Yu H, Wei P, Wu X, Zhu H, Gao H, Liang J, Li G; Yang W, 2019, UDP-glucose accelerates SNAI1 mRNA decay and impairs lung cancer metastasis, Nature, 571(7763): 127-131.
[26] Gao L, Chen X, Wang Y, Zhang J, 2020, Up-Regulation of FSTL3, regulated by lncRNA DSCAM-AS1/miR-122-5p Axis, promotes proliferation and migration of non-small cell lung cancer cells, Oncotargets and Therapy, 13: 2725-2738.
[27] Lei K, Liang R, Tan B, Li L, Lyu Y, Wang K, Wang W, Wang K, Hu X, Wu D, Lin H, Wang M, 2023, Effects of lipid metabolism-related genes PTGIS and HRASLS on phenotype, prognosis, and tumor immunity in lung squamous cell carcinoma, Oxid Med Cell Longev, 2023:6811625.
[28] Labat-de-Hoz L, Rubio-Ramos A, Correas I; Alonso M A, 2023, The MAL family of proteins: normal function, expression in cancer, and potential use as cancer biomarkers, Cancers, 15(10): 2801.
[29] Zhou M, Chen Y, Gu X, Wang C, 2022, A comprehensive bioinformatic analysis for identification of myeloid-associated differentiation marker as a potential negative prognostic biomarker in non-small-cell lung cancer, Pathology & Oncology Research, 28: 1610504.
[30] Suzuki J, Aokage K, Neri S, Sakai T, Hashimoto H, Su Y, Yamazaki S, Nakamura H, Tane K, Miyoshi T, Sugano M, Kojima M, Fujii S, Kuwata T, Ochiai A, Tsuboi M; Ishii G, 2021, Relationship between podoplanin-expressing cancer-associated fibroblasts and the immune microenvironment of early lung squamous cell carcinoma, Lung Cancer, 153: 1-10.
[31] Zhang H, Zhu Z, Modrak S, 2022, Tissue-resident memory CD4 + T cells play a dominant role in the initiation of antitumor immunity, Journal of Immunology, 208: 2837-2846.
[32] Xiang H, Ramil C P, Hai J, Zhang C, Wang H, Watkins A A, Afshar R, Georgiev P, Sze M A, Song X S, Curran P J, Cheng M, Miller J R., Sun D, Loboda A, Jia Y, Moy L Y, Chi A;

DOI: 10.54254/2753-8818/35/20240933

Brandish P E, 2020, Cancer-associated fibroblasts promote immunosuppression by inducing ROS-generating monocytic MDSCs in lung squamous cell carcinoma, Cancer Immunology Research, 8: 436-450.

[33] Paz-Ares L, Vicente D, Tafreshi A, Robinson A, Parra H S, Mazieres J, Hermes B, Cicin I, Medgyasszay B, Rodriguez-Cid J, Okamoto I, Lee S, Ramlau R, Vladimirov V, Cheng Y, Deng X, Zhang Y, Bas T, Piperdi B; Halmos B, 2020, A randomized, placebo-controlled trial of pembrolizumab plus chemotherapy in patients with metastatic squamous NSCLC: protocol-specified final analysis of KEYNOTE-407, Journal of Thoracic Oncology, 15: 1657-1669.